DETECTORS FOR QUARK AND GLUON JETS AT HIGH ENERGIES

B.H.Wiik

II.Institut für Experimentalphysik, Univ.Hamburg, and
Deutsches Elektronen-Synchrotron DESY, Hamburg.

Introduction

During the past two decades, theory and experiments have conspired to produce a cohesive and simple picture of nature. At least down to distances of 10^{-16} cm, matter is made of two kinds of pointlike fermions, leptons and quarks arranged in three families:

$$\left[\begin{pmatrix}\nu_e\\ e\end{pmatrix}\ \begin{pmatrix}u\\ d\end{pmatrix}\right]\quad\left[\begin{pmatrix}\nu_\mu\\ \mu\end{pmatrix}\begin{pmatrix}c\\ s\end{pmatrix}\right]\quad\left[\begin{pmatrix}\nu_\tau\\ \tau\end{pmatrix}\ \begin{pmatrix}-\\ b\end{pmatrix}\right]$$

Although the last family is not yet complete, the observed properties[1] of the b quark strongly favours the existance of a (2/3e) charged t quark.

The leptons have electromagnetic and weak interactions and are directly observed as free particles. The quarks have colour (strong charge) and participate in the strong interaction. So far, only colour singlets i.e. hadrons made of two or three quarks have been observed in abundance. This has led to the conjecture that quarks are confined and do not appear as free particles.

The forces, strong, electromagnetic and weak are predicted to arise from the exchange of gauge bosons. The best known force, the electromagnetic force arise from the exchange of a photon. The charged and neutral weak force is mediated by the exchange of the $W^{\pm}$ and the Z^0 gauge bosons. It has been proposed[2] that the electromagnetic and the weak forces are unified to an electroweak interaction on a mass-scale of 100 GeV/c^2. This conjecture has been strikingly confirmed by the discovery[3] of the $W^{\pm}$ and Z^0 boson at the CERN $p\bar{p}$ collider.

The leading candidate for a field theory of strong interaction is at present Quantum Chromo-Dynamics[4] (QCD). In QCD, the strong force is mediated by eight massless coloured vector particles, gluons, which couple directly to colour. The strong coupling constant α_s is independent of quark flavour, but depends on Q^2, the momentum transfer squared in the process. This results in a coupling which is strong at small values of Q^2 (large separations) and "weak" at large values of Q^2 (small separations). The Q^2 dependence of the coupling constant reflects the fact that gluons are coloured objects with self interaction. The first[5] indirect evidence for the existence of gluons came from deep inelastic lepton-nucleon experiments. Electron-positron interactions have given direct evidence[5] for gluons both from the observation of quark-gluon bremsstrahlung and from a study of the decay of heavy quarkonium states.

A struck quark or a radiated gluon does not appear as a free particle in the laboratory but rather as a jet of hadrons clustered around the initial direction of the parton.

To continue our study of fundamental constitutents we must piece together the initial parton state from a measurement of the final state hadrons even though the transformation of a quark into a jet of hadrons is not understood. The purpose of my talk is to discuss how this may be done. Before I get to the main topic, however, I would like to briefly review the experimental properties of jets as observed in e^+e^- collisions.

Properties of hadron jets

Due to its simplicity electron-positron annihilation is well suited to study the properties of hadron jets. In lowest order e^+e^- annihilate to a timelike electroweak current which couples directly to the basic fermions as shown in Fig. 1a. This picture is correct since at the short distances (small compared to 10^{-14} cm) involved in present e^+e^- interactions we may consider quarks and gluons as unconfined. As the quarks start to move apart, the potential between the quarks increases and new quarks are pairproduced from the vacuum. The quarks are also retarded by the colour field and radiate gluons. At distances large compared to 10^{-13} cm the quarks coalesce into colourless hadrons, resulting in two accolinear hadron jets.

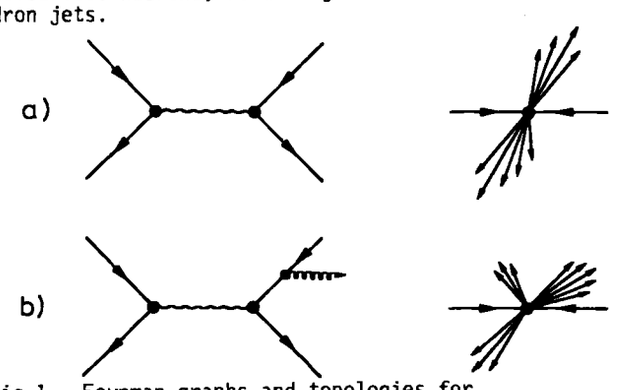

Fig 1 - Feynman graphs and topologies for
a) $e^+e^- \to q\bar{q}$ b) $e^+e^- \to q\bar{q}g$

The outgoing quark may also radiate a gluon at a large angle resulting in three well separated hadron jets as indicated in Fig.1a. Examples of two and three jet events as observed at PETRA are shown in Fig. 2a and 2b.

The transition from a struck quark to a jet of hadrons is a non perturbative process and is not well understood. However, the following features[6] seem to be supported by experiment:

- direction and energy of the primary quark is related to the direction and energy of the hadron jet.
- the quark-gluon branching process is flavour neutral ($u\bar{u}$, $d\bar{d}$, $s\bar{s}$ -) and the flavour of the jet is carried by the hadron containing the primary quark. In all fragmentation models pair-production of heavy quarks from the vacuum is strongly suppressed.
- The hadron containing the primary quark is on average found at large values of $x = E_h/E_b$ where E_h is the energy of the hadron and E_b is the beam energy. This is true even for the pairproduction of light quarks. For heavy primary quark it is favoured by kinematic arguments.

We will now briefly review the properties[5,6] of jets as they appear at PETRA and PEP energies:

The jet structure is generally analyzed in terms of sphericity[7] or thrust[8]. The sphericity S is defined as:

$$S = 3/2 \min \left[\Sigma_i (p_T^i) \,/\, \Sigma (p^i)^2\right]$$

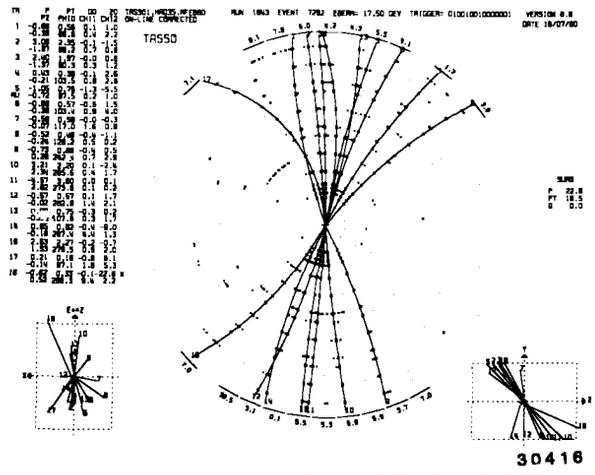

Fig. 2a - Two jet event observed by the TASSO group at PETRA. The event is viewed along the beam direction.

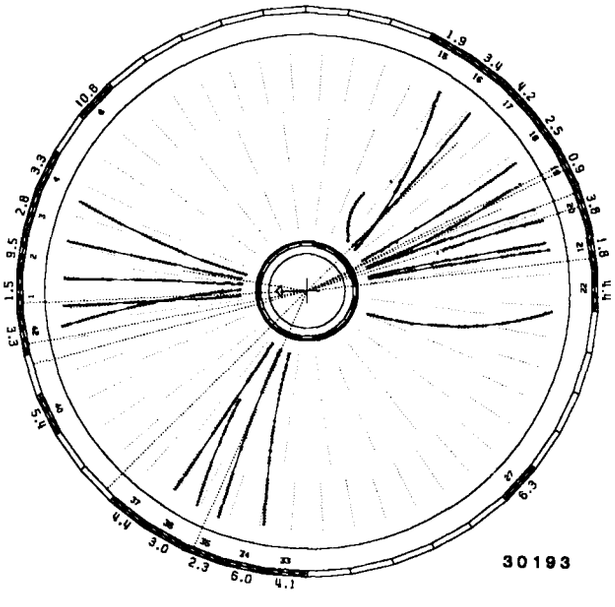

Fig. 2b - Three jet event observed by the JADE group at PETRA. The event is viewed along the beam direction.

Here p^i is the momentum and p_T^i the transverse momen- of a track with respect to a given axis. The jet axis is defined as the axis which minimizes transverse momentum squared. Sphericity measures the square of the jet cone half opening angle

$$S = 3/2 \; \langle \delta^2 \rangle$$

The average sphericity measured by TASSO at PETRA is plotted versus c.m. energy W in Fig.3. The sphericity was evaluated for each hemisphere independently. After a initial rapid decrease the sphericity seems to flatten out at a value of $S = 0.1$ corresponding to $\delta \sim 15°$. The energy dependence of S can be explained by gluon bremsstrahlung producing multiple jets in one hemisphere. If we evaluate the sphericity for single jets we find that the opening angle δ decreases as:

$$\delta \simeq \frac{0.35 \text{ GeV/c}}{\langle p \rangle}$$

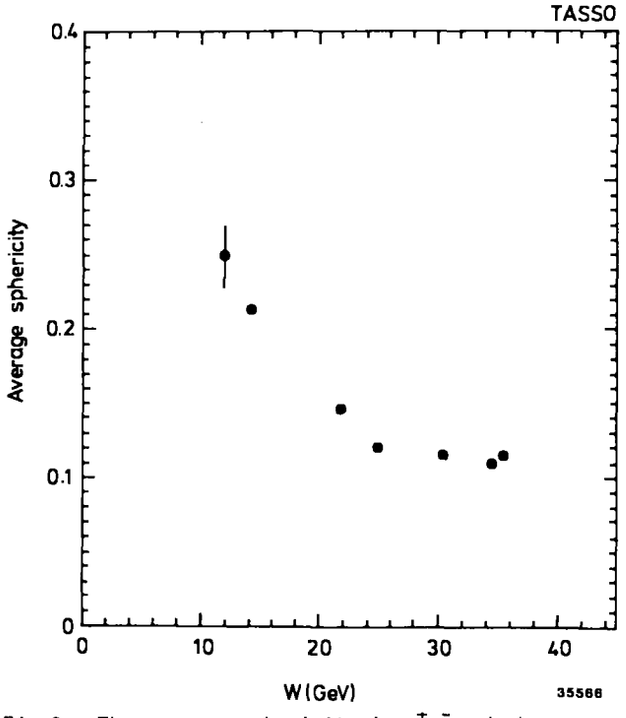

Fig 3 - The average sphericity in e^+e^- → hadrons plotted as a function of c.m. energy. The data are from the TASSO group at PETRA.

<p> is the average momentum of a hadron in a jet.

The gross properties of the hadrons in a jet can be summarized as follows:

- about 60% to 65% of the total energy in a jet is carried by charged particles. This ratio changes little with energy between 10 and 40 GeV in c.m.
- The mean charged multiplicity $\langle n_c \rangle$ observed in e^+e^- annihilation is plotted in Fig.4. The multiplicity rises rapidly and is well fit to the QCD prediction

$$\langle n_{ch} \rangle = a + b \exp \{c(\ln s/\Lambda^2)^{1/2}\}$$

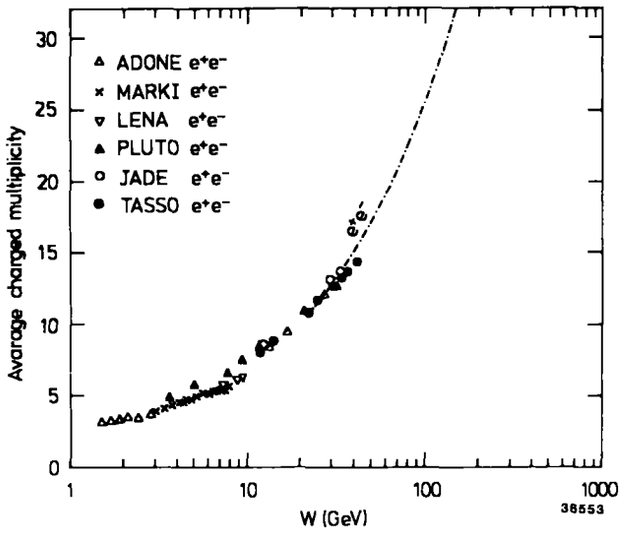

Fig. 4 - The average charged multiplicity observed in e^+e^- → hadrons is plotted as a function of c.m. energy. The curve represents a QCD fit of the form above.

The fit, with the assumption $\Lambda = 0.2$ GeV yields $a = 2.36 \pm 0.11$, $b = 0.0066 \pm 0.0018$ and $c = 2.31 \pm 0.09$.

- The average momentum of a charged track observed in e^+e^- annihilation is plotted in Fig. 5 versus energy. The function $\langle p \rangle = 0.60\ W/\langle n_c \rangle$ is shown as the solid line.
- At a c.m. energy of 35 GeV an average event consists of 10.3 π^-, 6.1 π^0, 2.0 K^-, 1.6 $K^0(\bar{K}^0)$ and 0.8 $p\bar{p}$. Also the particle ratio does not seem to change strongly with energy above the $b\bar{b}$ threshold.

An extrapolation of the charged multiplicity and the mean momentum of a charged particle are also shown in Figs. 4 and 5. At a c.m. energy of 200 GeV we expect a mean charged multiplicity of 38 and the charged particles have a mean momentum of 3.2 GeV/c^2.

A struck quark will in general produce hadrons within a cone of full opening angle $2\delta = 30°$. However, the angular width of a single jet excluding hard gluon bremsstrahlung, will shrink as $2\delta = 0.7$ GeV/$\langle p \rangle$. Thus at high energies multiple jet production will become visible.

A 4 jet event observed at PETRA is shown in Fig.6.

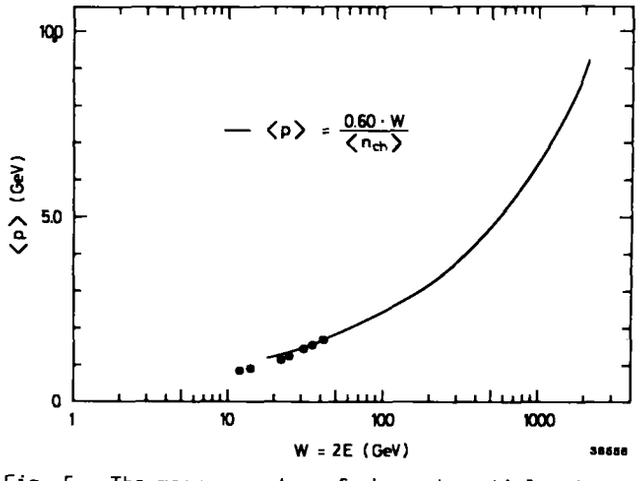

Fig. 5 - The mean momentum of charged particles in e^+e^- → hadrons is plotted as a function of c.m. energy. The data are from TASSO. The curve represents

$$\langle n_{ch} \rangle = \frac{0.60 \cdot W}{\langle n_{ch} \rangle} .$$

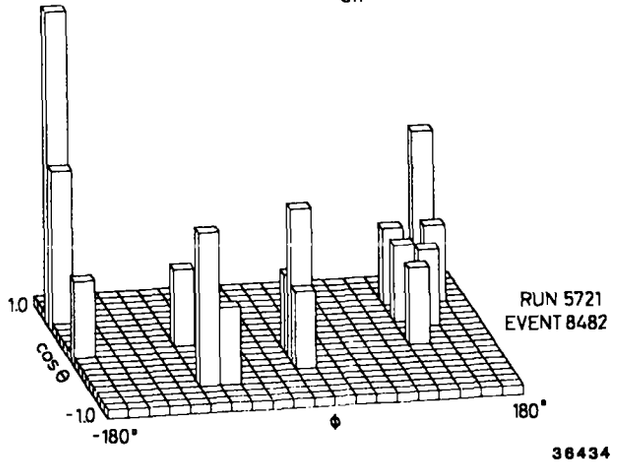

Fig. 6 - Four jet event observed by TASSO at PETRA.

Parton kinematics

To reconstruct the parton kinematic we need to measure the amount of energy, charged and neutral, emitted in a solid angle element $\Delta\Omega$ along the direction θ, φ. The size of a solid angle element should be small compared to $(0.70\ \text{GeV}/\langle p \rangle)^2$ which is a measure of the solid angle occupied by a "naked" jet. This implies that for a jet of $Q^2 = 10^4$ $(\text{GeV}/c)^2$ the full solid angle of 4π should be subdivided into 10^4 elements. The energy resolution should also be optimized. As an example, we may reconstruct the kinematic of the reaction $e\ p \to \nu\ X$ from a measurement of the current jet. In the central region the resolution in Q^2 and ν is always limited by the energy resolution.

Measurements of the energy flow can be done using either magnetic spectrometers surrounded by electro- magnetic calorimeters or by finely grained calorimeters.

Solenoids with the magnetic field oriented parallel to the beam direction are in almost universal use at the e^+e^--colliders. Charged particle tracking is done by various types of chambers - driftchambers, Time Projection Chambers etc, installed in the magnetic volume of the solenoid. Let us consider a particle of momentum p (GeV/c) emitted at 90° with respect to the beam axis. The particle traverses a detector of radius R(m) and its position in the bend plane is measured with an accuracy of σ(m) at n equidistant points. The axial magnetic field is of strength B(T). The fractional momentum error[9] resulting from measurement errors only is then given by:

$$(\Delta p_\perp / p_\perp)_\varepsilon = \frac{90}{\sqrt{n}} \frac{\Delta p_\perp}{BR^2}$$

The multiple scattering suffered by the particle traversing the detector results in a momentum error:

$$(\Delta p/p)_{m.s.} = \frac{0.116}{BR} (t)^{1/2}$$

t is the total thickness of material traversed by the particle measured in units of a radiation length.

At high momenta $\Delta p/p$ is dominated by measurement errors. Let us assume a particle of momentum p = 10 GeV/c traversing a detector with R = 1.5 m, B = 1.5 T, n = 20, and σ = 200 μm. In this case $\Delta p/p = 1.2 \cdot 10^{-3} p$.

In ep colliders and $p\bar{p}$ (pp) colliders the produced particles tend to travel at small angles with respect to the beam axis. Furthermore the mean particle momentum will be appreciable higher than those produced at PETRA and PEP (Fig. 5). Both factors tend to favour a finely grained calorimeter to measure the energy flow. So far the best results on the measurements of hadronic energy have been obtained[10] using Uranium plates immersed in liquid Argon. A fractional resolution of

$$\Delta E/E = \frac{Q30}{\sqrt{E}}$$

has been reported[10] for a calorimeter made of 1.7 mm thick U^{238}-plates in liquid argon. The spacial resolution σ_x can be written[10] as:

$$\sigma_x = 1.0 \exp(1.2\ s/\lambda) \quad \text{(in cm)}$$

Here s and λ are, respectively, the calorimeter-segmentation and the effective interaction length.

Even for a perfect detector several problems arise when we want to determine the parton kinematic from a measurement of the hadronic final state.

- each observed track must be assigned to a jet. Several alogorithms, sphericity, thrust etc. are in use. Monte Carlo calculations indicate that the error on the jet direction from this source is on the order of a few degrees.
- A theory which describes the transformation of a struck parton into a jet does not exist. For example in the Lund model[11] partons are connected with strings and the strings fragment as a whole. In this case the jet direction does not coincide directly with the parton momentum.

As an example of how to reconstruct the initial state from a measurement of the final state jets we will briefly discuss the results[12] of a Monte Carlo calculation of the process $e^+e^- \to H^0Z^0 \to$ (2 jets) (2 jets) as seen in the ALEPH detector[13]. The reaction was studied at a c.m. energy of 160 GeV and the mass of the Z^0 and H^0 taken to be 89 GeV and 50 GeV respectively. The topology of the process is dominated by 4 jet events.

Charged final state particles are measured with an assumed momentum resolution $\Delta p/p = 1.2 \cdot 10^{-3}\ p$. Photons are measured[13] by a calorimeter.

The observed particles are grouped into 4 jets using the generalized sphericity method[14]. The direction of the jet is given by the vector sum of all particles assigned to that jet. The jet velocity is defined as the velocity of the group of particles assignmed to the jet:

$$\vec{\beta}_{jet} = \vec{\beta}_{group} = \vec{p}_{group} / E_{group}$$

The energies of the jets are determined from momentum-energy conservation:

$$\sum_i E_{jet\ i}\ \vec{\beta}_{jet\ i} = 0$$

$$\sum_i E_{jet\ i} = E_{c.m.}$$

The following cuts were made to enhance the signal to background:

i) sphericity > 0.3

ii) minimum (maximum) opening angle between any two jets > 30° (< 166°).

The jets are ordered such that the invariant mass between jet 1 and jet 2 gives a mass (M_{12}) closest to the input Z^0 mass. The remaining jets are then candidates for the decay $H^0 \to b\bar{b}$. For events with 80 GeV/c^2 < M_{12} < 100 GeV/c^2, M_{12} is constrained to be 89 GeV/c^2 and the effective mass M_{34} between jet 3 and jet 4 is evaluated with this constraint.

The invariant mass distribution M_{34} is plotted in Fig. 7. A clear peak on top of a smooth QCD background is seen near the assumed mass of the H^0. The signal to background is about 1 : 1.

Note that a H^0 of mass 50 GeV/c^2 is expected to decay almost solely into $b\bar{b}$. Thus if we could identify the flavor of the jets the background will be reduced to a negligible level. How this might be done will be discussed in the next section.

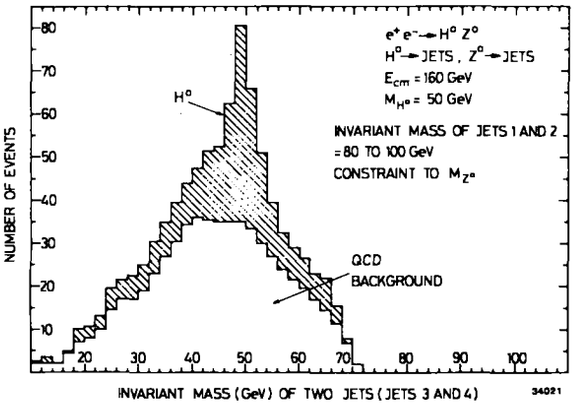

Fig. 7 - Results of a Monte Carlo calculation of the process $e^+e^- \to Z^0H^0 \to$ (2 jets) (2 jets). Plotted is the invariant mass distribution M_{34} from a measurement of jet 3 and 4. M_{12} from jet 1 and 2 is constrained to the assumed Z^0 mass.

Flavour tagging

Is it possible to reconstruct the flavor of the initial quark from a measurement of the hadrons in the final state ? This can be tested by looking for charge correlations between back to back produced jets in e^+e^- annihilation. The back to back produced quarks in e^+e^- annihilation have opposite charge and according to the standard picture they will fragment into hadrons by a neutral quark-gluon cascade conserving the initial charge. Therefore, apart from fluctuations, the resulting jet should remember the charge of the primary quark, so that the charge found in one jet should be correlated with the charge of the other jet. Furthermore one expects this long range correlation to be found among the fast particles, and that the slow particles should display short range correlations only. The TASSO group at PETRA has found evidence[15] for those correlations.

The charge correlation has been investigated by evaluating the function:

$$\bar{\Phi}(y,y') = -\frac{1}{\Delta y \Delta y'} (1/n \sum_{k=i}^{n} \sum_{i \neq k} e_i(y) e_k(y')).$$

In this expression $e_i(y)$ is the charge of a particle i at rapidity y in the interval Δy, and $e_k(y')$ is the charge of a particle k at a rapidity y' in the interval $\Delta y'$. The rapidity is defined as

$$y = \frac{1}{2} \ln [(E + p_{\parallel}) / (E - p_{\parallel})] .$$

where $p_{\parallel}$ is the particle momentum along the jet axis. The function $\bar{\Phi}(y,y')$ is related to the probability that the particles i and k have opposite-sign charges minus the probability that the charges have the same sign. Since the event as a whole is neutral, the function $\bar{\Phi}(y,y')$ simply shows how the charge of particle i at rapidity y is being compensated. The normalization is chosen such that $\int\bar{\Phi}(y,y')dy' = 1$. In Fig. 8 the ratio $\bar{\Phi}(y,y') = \int\bar{\Phi}(y,y')/\int\Phi(y,y')dy$ is plotted versus y with the test particle in various rapidity intervals y'.

The distribution for $-0.75 < y' < 0$, i.e. a slow particle, is shown in Fig. 8. This distribution peaks at small negative values of y and shows that the charge of a slow particle is indeed compensated locally, as expected if only short range correlations are present. The data are in good agreement with the

standard Monte Carlo calculations (see below) based on $q\bar{q}$ and $q\bar{q}g$ production shown as the solid line.

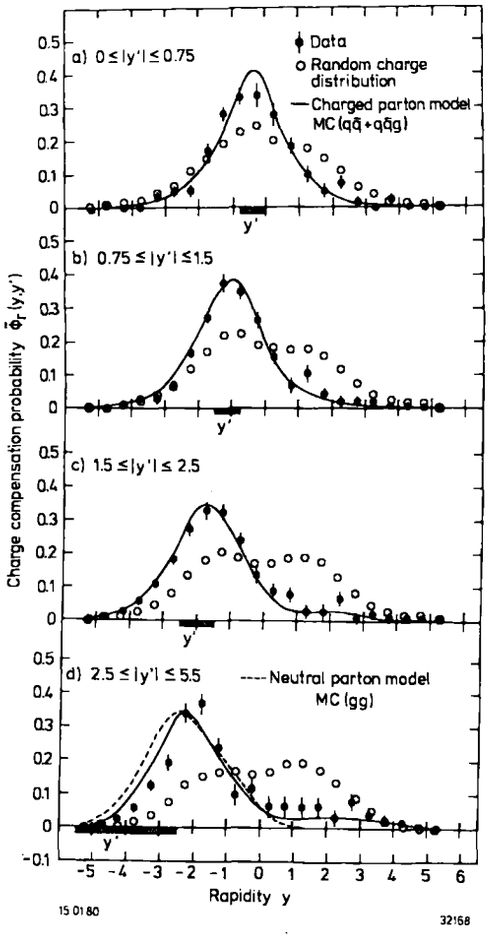

Fig. 8 - The charge compensation probability plotted versus rapidity y for various rapidity intervalls $\Delta y'$ of the test particle. The prediction for a charged and neutral parton model is shown by the solid and the dashed line. The charge compensation probability for a randomized charge distribution is shown by the open circles. The data were obtained by TASSO.

As the test particle becomes faster the distribution becomes increasingly skewed with a tail extending to positive y values. In Fig. 8 the correlation function is plotted for $-5.5 < y' < -2.5$. Although the bulk of the charge is still compensated locally, there is now a significant signal at the opposite end of the rapidity plot. The probability that the charge of a particle with $y' < -2.5$ is compensated by a particle in the opposite jet with $y > 1$ is $(15.4 \pm 2.6)\%$.

This long range correlation is also reproduced by the standard Monte Carlo program. However, this correlation is not present if the initial partons are neutral. This was demonstrated by using the same Monte Carlo program, but assuming the initial quark to be neutral. The results, shown as the dashed line in Fig. 8 fail to reproduce the long range correlation observed.

The charges were also distributed at random among the particles in an event and the resulting correlation function evaluated. The ensuing correlation functions, shown as the open circles are much wider than the data. Thus the TASSO group has demonstrated that a long range charge correlation between particles in opposite jets exists and that the initial partons are charged.

To determine the jet flavour one must identify the hadron containing the primary quark. The charge correlation data show that the "flavour" carrying hadron is most frequently found at large values of $x = E_h/E_b$. For a heavy primary quark this is basically a kinematic effect[16] - the heavy quark is only slightly retarded as it combines with a light quark from the sea to form a colourless meson. Pairproduction of heavy quark pairs from the sea is strongly suppressed. Therefore if we identify a hadron containing a heavy quark ($m_q > m_c$) then the hadron either contains the primary quark or it is the decay product of an even heavier quark.

The heavy quark will decay either into a mixed lepton-hadron final state $Q \to (\ell\bar{\nu}_\ell)q'$ or into a state containing only hadrons $Q \to (q\bar{q})q'$. In the spectator model the heavy quark decays independently of its partner and to a first approximation the decay widths, neglecting phase space, are given by:

$$\Gamma(Q \to (\ell\bar{\nu})q') \cdot |V_{Qq'}|^2 =$$

$$\frac{1}{3}\,\Gamma(Q \to (q\bar{q})q') \cdot |V_{Qq'}|^2 =$$

$$\left(\frac{m_Q}{m_\mu}\right)^5 \Gamma(\mu \to (e\nu)\nu)$$

$V_{Qq'}$ are the elements of the mixing matrix[17]. These matrix elements are near one for Q = 2/3e quark and small for Q = -1/3e quark. The factor 1/3 is due to colour counting. The main decay modes according to the standard model are shown in Fig.9.

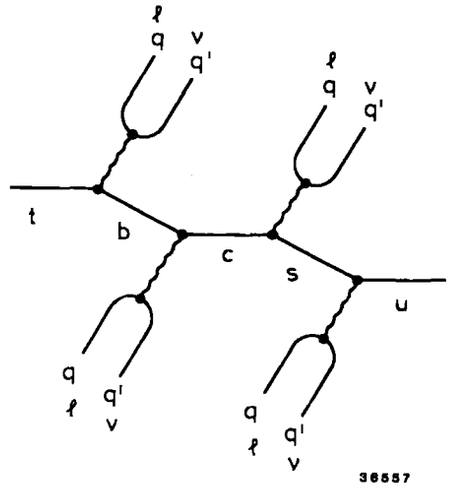

Fig. 9 - The main decay modes of a heavy quark according to the standard model.

From the decay pattern discussed above we may consider the following methods for flavour tagging. These methods are of course not exclusive and might be used in parallel.

1. Reconstruct the hadron containing the primary quark from its decay products.

In general the decay of a heavy hadron leads to a final state of high charged and neutral multiplicity resulting in a severe combinatiorial background. Only a small fraction of the produced hadrons will be seen if the search is restricted to low multiplicity modes.

As an example let us consider the discovery [18] of b- flavoured mesons at the CESR colliding ring at Cornell. The CLEO group at CESR collected data at the $\Upsilon(4s)$ peak which is known to decay nearly exclusively into $b\bar{b}$ pairs. The integrated luminosity of 40.7 pb^{-1} corresponds to some 82000 produced b-flavoured hadrons.

The b-quark is known to decay mainly into the c-quark leading to a final state consisting of a charmed meson and pions. To minimize the combinatiorial background the search was restricted to low multiplicty decay modes, D^0 or $D^{*\pm}$ plus one or two charged pions.

The effective mass distribution for the channels (plus charge conjugated) : $B^- \to D^0\pi^-$, $\bar{B}^0 \to D^0\pi^+\pi^-$, $\bar{B}^0 \to D^{*+}\pi^-$, $B^- \to D^{*+}\pi^-\pi^-$ are plotted in Fig.10 for events on the $\Upsilon(4s)$ resonance. They observe a clear peak centered at 5272.3 ± 1.5 ± 2.0 MeV/c^2 containing some 18 events. To estimate the background they changed the selection criteria for the $K^+\pi^-$ combination to give a mass which differs from the D^0 mass by ± 200 MeV/c^2. The spectrum of reconstruced "B meson" masses using this mass combination are also shown. The mass distribution shows no peaking at a particular mass value. From this and other methods they estimate the background to contribute between 4 and 7 events under the peak.

Although the existence of the b-flavoured meson is clear, the efficiency for its detection is rather low. Indeed, from the number above they find

$$\varepsilon = \frac{\text{Detected b-flavoured hadrons}}{\text{Produced b-flavoured hadrons}} \approx 1.5 \cdot 10^{-4}.$$

The efficiency can clearly be improved by incorpoating neutral detection and by improving particle identification and momentum resolution. However, it seems unlikely that this method will be useful to determine flavour on a jet to jet basis.

Experimentally it is very demanding to reconstruct a heavy hadron from its decay products. Besides good momentum resolution for charged particles and photons it requires particle identification over a wide range in momenta.

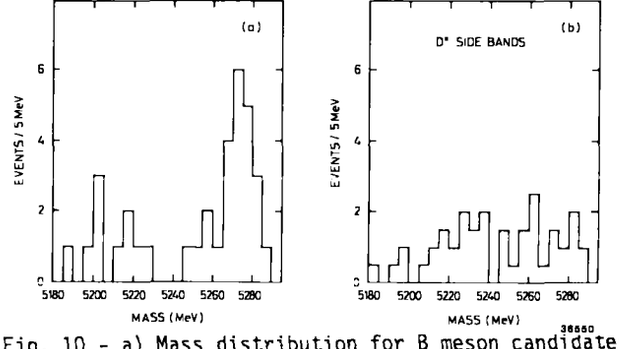

Fig. 10 - a) Mass distribution for B meson candidates observed in $e^+e^- \to \Upsilon(4s) \to (D^0n\pi)X$. The data are from the CLEO Collaboration at CESR b) Mass distribution with the D^0 chosen from side bands.

2. Determine the effective mass of a jet.

The flavour of heavy quarks produced not far from threshold can be determined from a measurement of the effective mass of a jet. As an example the effective mass distribution [19] for the fragmentation of a b or t quark with $Q^2 = 10^4$ (GeV/c)^2 is plotted in Fig. 11. The mass of the b- respectively the t-quark was chosen as 5 GeV/c^2 and 30 GeV/c^2. Gluon bremsstrahlung was included in the calculation. The reconstructed mass of the b-jet is centered around 18 GeV with a long tail extending to high mass. the effective mass of the jet is thus determined by gluon bremsstrahlung and, indeed, replacing the b quark with the light u-quark do not change the distribution appreciably. However, the mass distribution resulting from t-quark fragmentation is centered at 38 GeV and is well separated from the b-quark mass distribution. A measurement of the jet mass distribution can thus be used to identify a 30 GeV t-quark (up to c.m. energies of at least 100 GeV) but cannot discriminate between the b-quark and the lighter quarks at high energies. This is also true for other kine tic quantities like thrust, transverse mass etc. Such measurements can be carried out using a finely grained calorimeter or a magnetic detector incorporating a photon calorimeter.

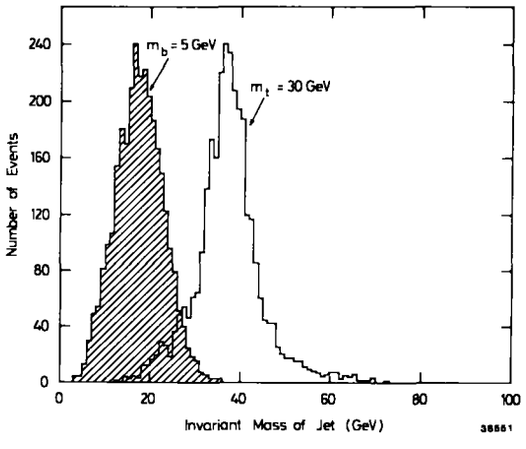

Fig. 11 - The computed invariant mass distribution from b → hadrons, t → hadrons with the assumed masses m_b = 5 GeV/c^2 and m_t = 30 GeV/c^2. The b and t are fragmented according to the standard Feynman-Field model.

3. Observe mixed lepton-hadron events.

This is a signature of the weak decay of a heavy quark. A limit on the quark mass is obtained from a measurement of the transverse momentum of the lepton with respect to the jet axis. This method has been used in several e^+e^- experiments to identify weakly decaying hadrons.

Data on inclusive electron events [20] obtained by the MARK II Collaboration at PEP are shown in Fig.12. Plotted is the lepton momentum spectrum for various cuts on its transverse momentum with respect to the jet axis. The prompt leptons may arise from $b \to e^-X$, $b \to c \to e^-X$ and $c \to e^-X$. The results of a Monte Carlo calculation of the various contributions are also shown in Fig. 12. At low $p_\perp$ values $c \to e\,X$ dominates where the large $p_\perp$ data mainly result from $b \to e\,X$ decays.

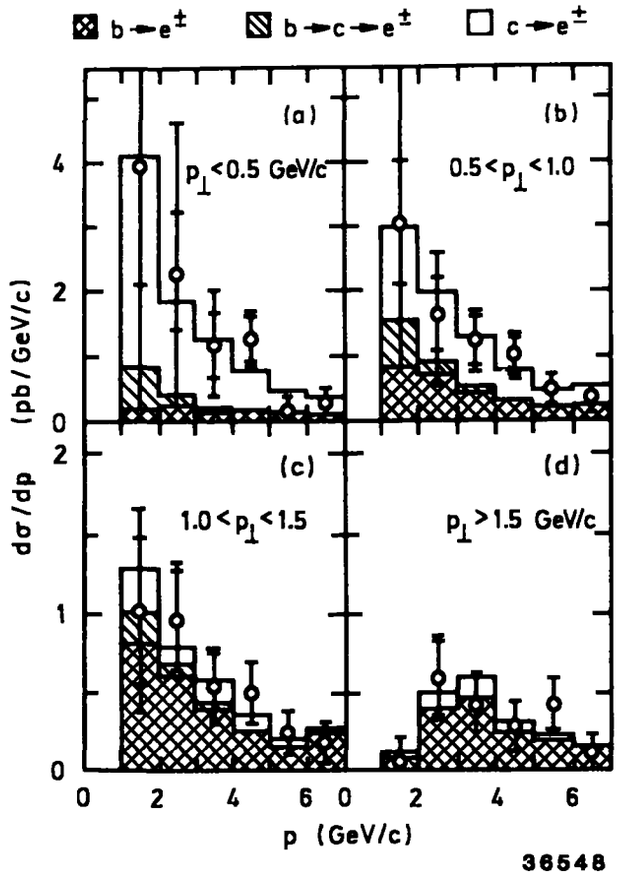

Fig. 12 - The cross section $d\sigma/dp$ for inclusive electron production is plotted as a function of momentum for various cuts on the transverse momentum with respect to the jet axis. The estimated contributions from $b \to e^{\pm} X$, $b \to c \to e^{\pm}X$ and $c \to e^{\pm}X$ are also shown. The data were obtained by the MARK II Collaboration at PEP.

It is clear that this method has ambiguities. Furthermore the detection efficiency is limited by the leptonic branching ratios to:

$$< B_1 \ (b \to e \ \nu_e \ X) > \ \sim \ 11.5\%$$

$$< B_2 \ (c \to e \ \nu_e \ X) > \ \sim \ 6.5\%$$

This measurement requires the identification and momentum measurement of a lepton travelling within a jet of hadrons.

4. Observe the decay vertex.

The lifetime of a heavy quark is given by

$$\tau_Q = \left(\frac{m_\mu}{m_Q}\right)^5 \cdot \frac{B_e \cdot \tau_\mu}{|V_{Qq'}|^2}$$

where τ_μ is the muon lifetime and B_e is the electron branching ratio. Experimentally the lifetime of D^+ and D^0 are found[21] to be:

$$\tau_{D^+} = (8.2 \ ^{+\ 1.1}_{-\ 0.9}) \cdot 10^{-13}\text{s} \quad \text{and}$$

$$\tau_{D^0} = (3.9 \pm 0.4) \cdot 10^{-13}\text{s}.$$

New preliminary data from the MAC[22] and MARK II[23] detectors at PEP reports a b-lifetime on the order of 10^{-12}s. It is thus possible to identify a c- or b-flavored hadron by a measurement of its decay vertex.

The kinematic is defined in Fig.13. The distance travelled by a relativistic particle before decaying is proportional to $\gamma = E/m_H$, however, the opening angle of its decay product shrinks proportional to $1/\gamma$. The impact parameter δ defined in Fig.13 is therefore independent of momentum at relativistic energies. The PEP groups have shown that the decays $c \to (e\bar{\nu}_e)X$ and $b \to (e\bar{\nu}_e)X$ lead to values of δ on the order of 100 - 150 μm in e^+e^- annihilation.

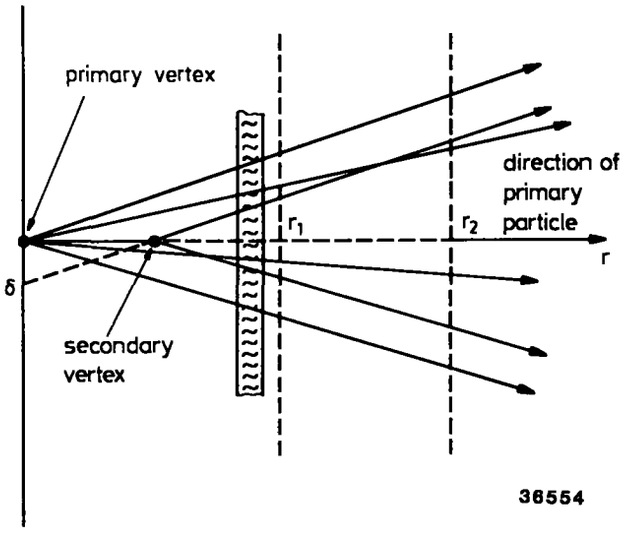

Fig. 13 - The detection of a secondary decay vertex using two silicon strip planes located at r_1 and r_2.

A resolution in δ of this order has been achieved using driftchambers with a spatial resolution of 100 μm. Solid state detectors like silicon strip detectors[24] or charged coupled devices[25] have the potential of a large improvement. As an example let us consider a silicon strip detector. Such detectors are now available in sizes of 50 x 50 mm^2, detector sizes of 70 x 70 mm^2 may become available in the future. The detectors can be bonded together to larger units. The detector is read out using a diode pattern covered by Aluminum contact strips on the surface of the crystal. The read out pitch may be on the order of 25 μm. These detectors, used in actual experiments[26] have achieved a rms resolution of 5 μm.

Assume that we measure the position of charged tracks with a precision of σ_1 and σ_2 in two silicon strip detectors located at a distance r_1 and r_2 from the interaction point. The first silicon strip plane is mounted adjacent to the beam pipe, and is the total thickness of beam pipe plus one silicon strip plane measured in units of a radiation length. The multiple scattering in the second plane can be neglected. The resulting error on δ is given by:

$$(\sigma_\delta)^2 = \frac{1}{(r_2 - r_1)^2}\,(r_2^2\,\sigma_1^2 + r_1^2\,\sigma_2^2) + r_1^2\ \langle\theta\rangle^2$$

with $\langle\theta\rangle = \frac{0.015\ \text{GeV}}{p}\sqrt{d}$.

For a nummerical value we assume that the planes are located at $r_1 = 3$ cm, $r_2 = 8$ cm, $\sigma_1 = \sigma_2 = 6\ \mu$ and $d = 6 \cdot 10^{-3}$. The impact parameter δ is obtained by a measurement of the position of the primary and the secondary vertex. In this case we determine δ with an error of 15μm and this would indeed make it possible to identify the majority of produced b and c quarks. The decays of b and c quarks can be separated in various ways, like observing multiple decay vertices, or from a measurement of transverse momentum.

It is tempting to use a silicon detector not only as a vertex detector but also as a tracking detector in a high field solenoid. Besides the high resolution the silicon detector has excellent two track resolution (< 50 μm), high rate capabilities (≤ 10^8 particles per second and strip) and it is not easily damaged by radiation.

A possible configuration[27] is shown in Fig.14. Three doublets of strip detectors are mounted in a solenoid field of induction B, L is the distance between the first and the last detector plane. The momentum resolution has been evaluated including multiple scattering in the beam pipe (1.5 mm Be) and in the six detector planes (300 μm Si/200 μm SiO_2). The result is plotted in Fig.14. The multiple scattering clearly dominates below 8 GeV/c. To determine $\Delta p/p$ we have to chose a value of B. Since the magnetic field volume is rather small it is possible to choose a high field of the order 8 Tesla. With $\sigma_c = 6\ \mu$ a 10 GeV/c track is measured with a resolution $\Delta p/p = 0.03$ only a factor of 2 worse than the resolution predicted for a large detector like ALEPH. However, much development is needed before such a detector can be realized.

It seems very likely that one will be able to identify t-, b- and c-quarks perhaps on an event by event basis. What about the lighter quarks ? Here the situation is much more difficult. For example a strange hadron may not only result from primary s-quark production but also from $s\bar{s}$ pairproduction from the vacuum or from the decay of heavier quarks.

In Fig. 15 the invariant cross section for inclusive $K^0 + \bar{K}^0$ and $K^+ + K^-$ production is shown. The estimated contribution from primary $s\bar{s}$, $c\bar{c}$ and $b\bar{b}$ production and from $s\bar{s}$ pair production from the vacuum together with the sum is also shown. Note that $s\bar{s}$ pair production from the vacuum will lead to K, $\bar{K}$ pairs adjacent in rapidity, primary $b\bar{b}$ and $c\bar{c}$ production may be identified directly using the methods discussed above. However, even so it looks like a formidable task to separate primary produced s-quarks from other sources.

Needless to say that the situation for u and d quarks is even more difficult.

The gluon and hence the resulting hadronic jet is flavour neutral. A gluon may fluctuate into pairs of gluons and quarks and this may lead to observable effects like a wider $p_\perp$ distribution from the hadrons and higher multiplicity. Such effects[28] have been reported from a study at PETRA. These are also indications[29] that a gluon jet may contain more baryons than jets resulting from the fragmentation of a quark.

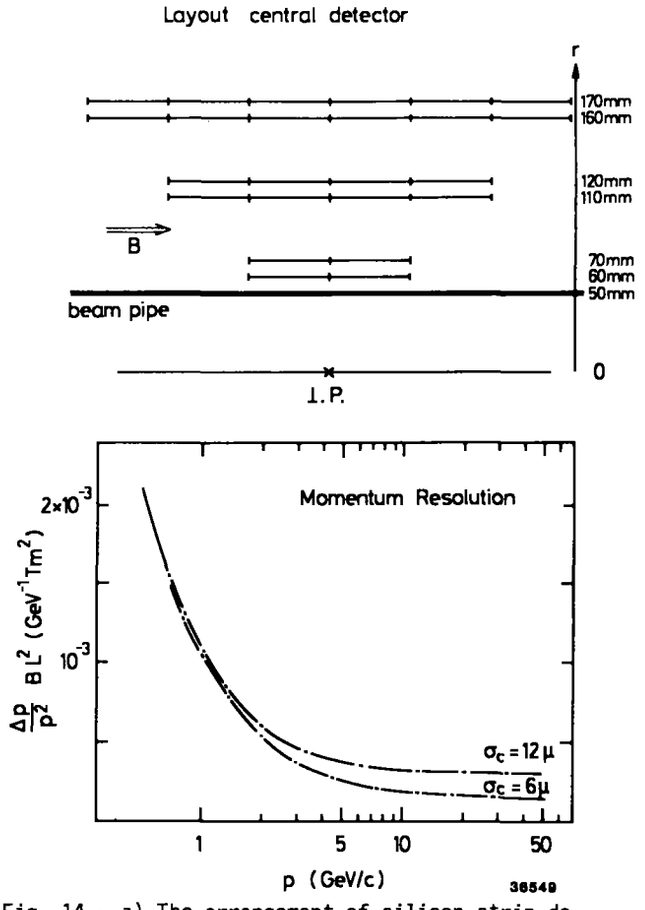

Fig. 14 - a) The arrangement of silicon strip detectors in a magnetic solenoid viewed transverse to the beam direction.

b) The momentum resolution including multiple scattering as a function of momentum for the detector shown above. The curves represent two different values of the intrinsic resolution.

To find a reliable signature for gluon jets we first need a source of unambigous gluon jets. The decays of bound states of the $t\bar{t}$ system is such a source either through

$$e^+e^- \to T(1^3S_1) \to 3\ g \quad \text{or} \quad \gamma gg$$

or through the decay

$$e^+e^- \to T(2^3S_1) \to \gamma\ ^3P_{2,0} \to \gamma gg$$

In concluding it seems rather likely that we will learn to determine the flavour of t-, b- and c-quarks initiated jets on an event to event basis. There might even be hope for s-quarks and gluon initiated jets. However, I leave it to the audience to ponder how they would identify the flavour of constituents inside the quark.

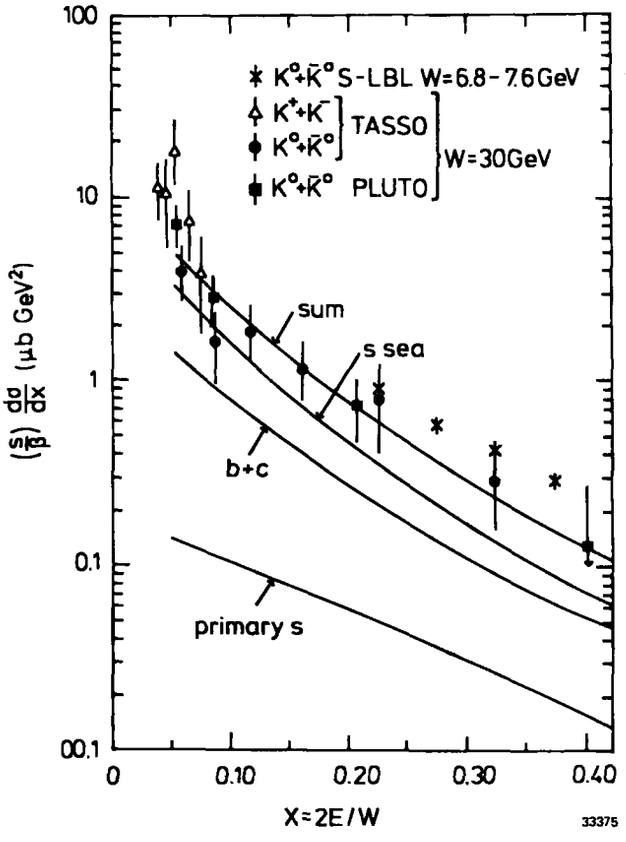

Fig. 15 - The invariant cross section $s/\beta\ d\sigma/dx$ for inclusive kaon production is plotted versus $x = 2E/W$. The estimated contributions from primary $s\bar{s}$, $c\bar{c}$ and $b\bar{b}$ production and from $s\bar{s}$ pair creation from the vacuum together with the sum is also shown.

References

1) K.Berkelmann, Lectures given at the 1983 Hawaii Topical Conference and references therein CCNS 83/581

2) S.L.Glashow, Nuclear Phys. 22, 579 (1961)
S.Weinberg, Phys.Rev.Lett.19, 1264 (1967)
A.Salam, Elementary Particle Theory, ed.
N.Svartholm (Almquist and Wiksell, Stockholm 1968, p. 361

3) UAI Collaboration, G.Arnison et al.,
Phys.Lett. 122 B (1983) 103,
UA2 Collaboration, M.Banner et al.,
Phys.Lett. 122 B (1983) 476,
UA1 Collaboration, G.Arnison et al.,
Phys.Lett. 126 B (1983) 398,
UA2 Collaboration, M.Banner et al.,
Phys.Lett. 129 B (1983) 130.

4) H.Fritzsch, M.Gell-Mann and H.Leutwyler,
Phys.Lett. 47B (1973) 365
D.J.Gross and F.Wilczek, Phys.Rev.Lett.30 (1973)1343
H.D.Politzer, Phys.Rev.Lett.30 (1973) 1346,
S.Weinberg, Phys.Rev.Lett. 31 (1973) 31.

5) For a recent review including references see:
K.H.Mess and B.H.Wiik in Les Houches Session XXXVII, 1981 in proceedings edited by
M.K.Gaillard and R.Stora, North Holland 1983

6) For a recent review of jet physics see:
G.Wolf, invited paper given at the 21st International Conference on High Energy Physics

6) continued
Published in Journal de Physique 43 (1982) 525.
P.Mättig, Talk given at the XVIIIth Recontre de Moriond, La Plaque-Savoie-France, 1983-038, 1983

7) E.Fahri, Phys.Rev.Lett. 39 (1979) 1587
S.Brandt and H.D.Dahmen, Zeit.Phys. C1 (1979) 61

8) J.D.Bjorken and S.J.Brodsky, Phys.Rev. D1 (1970) 1416.

9) R.L.Gluckstern, NIM 24 (1963) 381.

10) C.W.Fabjan et al., NIM 141 (1977) 61
S.R.Amendalia et al., Conference on Experimentation at LEP, Uppsala, June 1980.

11) B.Anderson, G.Gustafson and C.Petersen,
Nucl.Phys. B 135 (1978) 273

12) T.Barklow, G.Rudolph, S.L.Wu and H.Zobernig,
International ALEPH Note and private communication.

13) ALEPH Collaboration, Technical Report 1983

14) S.L.Wu, Zeit.Phys. C 9 (1981) 329

15) TASSO Collaboration, R.Brandelik et al.,
Phys.Lett. 100 B (1981) 357

16) J.D.Bjorken, Phys.Rev. D17 (1978) 171
M.Suzuki, Phys.Lett. 71B (1977) 189

17) M.Kobayashi and T.Maskawa,
Prog.Theor.Phys. 49 (1973) 652

18) CLEO Collaboration, S.Behrends et al.,
Phys.Rev.Lett. 50 (1983) 881

19) L.Day, private communication

20) M.E.Nelson et al., Phys.Rev.Lett.50 (1983) 1542

21) N.W.Reay, Invited talk at the 1983 International Symposium on Lepton and Photon Interactions at High Energies, Cornell Univ., August 1983

22) E.Fernandez et al., Phys.Rev.Lett.51 (1983) 1022

23) N.S.Lockyer et al., Phys.Rev.Lett.51 (1983) 1316

24) J.Kemmer, NIM 169 (1980) 449

25) See C.Damerell, FNAL Meeting on Semiconductor Devices in High Energy Physics, July 1981

26) B.Hyams et al., NIM 205 (1983) 99

27) P.G.Rancoita et al., HERA working group on Solid State Detectors, Amsterdam, June 1983
U.Kötz and R.Klanner private communication

28) JADE Collaboration, W.Bartel et al.,
DESY Report 83-080, 1983

29) EMC Collaboration, J.Aubert et al.,
Phys.Lett. 100 B (1981) 433
CLEO Collaboration, F.Pipkin et al.,
DASP Collaboration, H.Albrecht et al.,
Phys.Lett. 102B (1981) 291
DASP Collaboration, R.Brandelik et al.,
Nucl.Phys. B 148 (1979) 189.